ICARUS 115, 374–386 (1995)

Grain Sizes and Mineral Compositions of Surface Regoliths of Vesta-like Asteroids

TAKAHIRO HIROI[1]

SN3, NASA Johnson Space Center, Houston, Texas 77058
E-mail: hiroi@pggipl.geo.brown.edu

RICHARD P. BINZEL

Department of Earth, Atmospheric, and Planetary Sciences, Massachusetts Institute of Technology, Cambridge, Massachusetts 02139

JESSICA M. SUNSHINE

SETS Technology, Inc., 300 Kahelu Avenue, Mililani, Hawaii 96789

CARLÉ M. PIETERS

Department of Geological Sciences, Brown University, Providence, Rhode Island 02912

AND

HIROSHI TAKEDA

Mineralogical Institute, Faculty of Science, University of Tokyo, Hongo, Tokyo 113, Japan

Received August 4, 1994; revised December 1, 1994

Visible and near-infrared reflectance spectra (0.4–1.0 μm) of 21 Vesta-like asteroids and 12 HED meteorite powders (<25 μm in grain size) have been compared. Each reflectance spectrum was deconvolved into modified Gaussians and a constant background to allow comparisons of the 1-μm absorption band position and shape. The 1-μm band centers and widths of Vesta-like asteroids and HED meteorites generally overlap, but asteroids have a slightly wider range of band centers and widths indicating a wider range of Fe, Mg, and Ca content of their pyroxenes. Many of the Vesta-like asteroids, however, have shallower 1-μm absorption bands than HED meteorites. The weaker 1-μm band suggests that the surface regoliths of those asteroids may contain a larger amount of either fine grains or plagioclase than the laboratory-prepared HED meteorite powders. The most serious spectral difference between Vesta-like asteroids and HED meteorites is their visible absorption strength (reflectance drop-off shortward of ~0.7 μm) relative to the 1-μm band strength. Vesta-like asteroids tend to have stronger visible absorption than HED meteorites. The difference in the visible absorption strength may be due to some minor transition elements (Ti, Cr, etc.) in pyroxene, other unidentified mineral components, or space weathering processes. © 1995 Academic Press, Inc.

[1] Present address: Department of Geological Sciences, Brown University, Providence, Rhode Island 02912.

1. INTRODUCTION

Asteroid 4 Vesta had been the single asteroid whose surface mineralogy is well defined because its reflectance spectrum is very similar to a group of basaltic achondrites called HED meteorites (McCord *et al.* 1970). Additional reflectance spectra of Vesta were measured at various rotational phases, and its surface heterogeneity was detected (Gaffey 1983). Vesta-like asteroids were later found among the small asteroid population in near-Earth orbits (McFadden *et al.* 1984, Bell 1988, Cruikshank *et al.* 1991). Recently, 20 more small asteroids have been found to have Vesta-like reflectance spectra (Binzel and Xu 1993). They are located near Vesta's orbit and in between Vesta and the 3 : 1 Kirkwood Gap, which gives a possible genetic (dynamical) connection between Vesta and near-Earth Vesta-like asteroids and HED meteorites.

Existence of particulate regoliths on some asteroids has been detected and the grain-size distribution has been estimated by polarimetric studies (Dollfus *et al.* 1977, 1989). Le Bertre and Zellner (1980) compared the polarimetric and photometric properties of Vesta and an eucrite and concluded that Vesta's surface is well simulated by a broad mixture of particle sizes mainly >50 μm mixed and coated with particles <10 μm. Hiroi *et al.* (1994) showed that Vesta's spectral shape and albedo are well

0019-1035/95 $6.00

fit with a howardite powder of grain size <25 μm. It is of interest to study if small (<10 km in diameter) Vesta-like asteroids also have such fine particles in their surface regoliths.

In this paper, CCD reflectance spectra of the 21 Vesta-like small asteroids and the laboratory bidirectional reflectance spectra of 12 HED meteorite powders have been compared. The 1-μm band of their reflectance spectra is caused by the transitions between *d*-electron energy states of Fe^{2+} mainly in the M2 site of Ca-poor pyroxenes and in the M1 and M2 sites of Ca-rich pyroxenes (e.g., Rossman 1980). Therefore, comparing the 1-μm band-center wavelength, width, and strength between the Vesta-like asteroids and HED meteorites should give information about whether their pyroxene chemical compositions and the grain-size distributions are comparable.

2. OBSERVATIONAL AND EXPERIMENTAL PROCEDURES

Visible and near-infrared reflectance spectra of Vesta and 20 Vesta-like asteroids were measured by Binzel and Xu (1993) using a CCD detector. The wavelength resolution is about 1 nm covering different ranges from one asteroid to another, depending on the observational conditions (0.4–1.0 μm in the best case).

Fresh chips of seven eucrites (ALHA76005, ALH78132, Juvinas, Millbillillie, Padvarninkai, Stannern, and Y74450), a howardite (EET87503), and four diogenites (EETA79002, Johnstown, Y74013, and Y75032) were ground with a mortar and pestle and dry-sieved into powders of grain size <25 μm. The ranges of pyroxene Fe contents (Fs%) of these meteorites are listed in Table I. Bidirectional reflectance spectra of the 12 HED meteorite powders were obtained at every 5 nm from 0.48 to 1.0 μm using the RELAB facility with viewing geometry of 30° incidence and 0° emergence angles. The details of RELAB are described in Pieters (1983) and in the RELAB Users Manual.

TABLE I
Classifications and the Approximate Fe Contents (Fs%) of HED Meteorites

Meteorite	Class	Fs%	Reference
ALHA76005	Euc	37–57	1
ALH78132	Euc	40–68	1
Juvinas	Euc	35–60	4
Millbillillie	Euc	25–62	4
Padvarninkai	Euc	26–60	4
Stannern	Euc	26–62	4
Y74450	Euc	25–51	2
EET87503	How	20–56	1
EETA79002	Dio	22	1
Johnstown	Dio	22.6	3
Y74013	Dio	23.0–25.6	2
Y75032	Dio	29.1–34.7	2

Note. 1, Score and Lindstrom 1990; 2, Yanai and Kojima 1987; 3, Takeda *et al.* 1975; 4, Yamaguchi 1993 (personal communications).

3. METHOD OF COMPARING REFLECTANCE SPECTRA

Asteroid and meteorite reflectance spectra were converted to their natural logarithm and were deconvolved into a constant (flat) background and a series of modified Gaussians:

$$\log R(\nu) \cong f(\nu) = c_0 + \sum_{i=1}^{3} s_i \exp\left[-\frac{1}{2}\{(\nu^{-1} - \mu_i)/\sigma_i\}^2\right], \quad (1)$$

where $R(\nu)$ indicates the measured reflectance at wavenumber ν, and the band parameters μ, σ, and s shall be called the absorption-band center, half-width, and strength, respectively. The band center and half-width are in wavelength. This model is the same as the modified Gaussian model (Sunshine *et al.* 1990, Sunshine and Pieters 1993) except for the form of the background function. A constant background was chosen as continuum in order to minimize any influence on the calculated 1-μm band center values. The band strength s is always negative. The full width at half-maximum (FWHM) can be obtained from σ by

$$\text{FWHM} = 2\sqrt{2\log 2}\cdot\sigma = 2.35482\sigma \quad (2)$$

(e.g., Huguenin and Jones 1986), which will be simply called the band width. The parameters in Eq. (1) are optimized by minimizing the square deviation (ε) between the measured and calculated spectra,

$$\varepsilon = \sum_{i=1}^{N} \{\log R(\nu_i) - f(\nu_i)\}^2, \quad (3)$$

where ν_i indicates the wavenumber of the ith data point, and N is the total number of the data points. The quality of the deconvolution is measured by the root mean square deviation (RMSD):

$$\text{RMSD} = \sqrt{\varepsilon/N}. \quad (4)$$

Three modified Gaussians were used as the minimum number of functions necessary to fit the major absorption bands. As the initial value for the background, the minimum possible value was chosen, which was equal to the maximum natural log reflectance value near 0.74 μm. This method should give consistent absorption band center wavelengths. Band width and strength are more sensitive to the choice of the initial background value.

After deconvolving each asteroid spectrum by the above method, artificial random noise was added to the solution spectrum as a simulation of noise introduced during the observation of the asteroid, and the spectrum was deconvolved again to estimate the error ranges of the band parameters (center, width, and strength). The artificial noise was generated based on a normal (Gaussian) distribution with the same standard deviation between the observed and deconvolved spectra of the asteroid. The calculation was repeated 10 times in order to estimate the standard deviations of the band parameters.

Using spectra modeled by the above method, the relative strength of the visible absorption bands for Vesta-like asteroids and HED meteorites is estimated by the parameter, V,

$$V = \frac{\ln R_M - \ln R_{55}}{\ln R_M - \ln R_C}, \quad (5)$$

where R_{55}, R_M, and R_C indicate reflectance values of each modeled spectrum at 0.55 μm, at the maximum point near 0.74 μm, and at the 1-μm band center. The visible absorption strength in the numerator in Eq. (5) is normalized by the 1-μm band strength in the denominator to correct possible difference in grain size among the asteroids and the meteorites. The parameter V shall be simply called visible absorption strength. The standard deviations of the V values in Eq. (5) for the asteroids were estimated from their RMSD values in Eq. (4).

4. RESULTS OF COMPARISON

The deconvolved reflectance spectra of the Vesta-like asteroids are shown in Fig. 1, and the optimized 1-μm absorption band parameters are listed in Table II together with their error estimates. All the major broad absorption bands are well fit with three modified Gaussians and a flat background. The residual error spectrum is shown in the top part of each plot in Fig. 1. High-quality reflectance spectra (such as Vesta, Kollaa, Mourao, and 1978 ST6) are especially well deconvolved. The systematic errors around wavelengths 0.72, 0.82, and 0.91 μm for many asteroids (1273, 1906, 3155, 3268, 3869, 4005, 4038, 4215, etc.) are probably due to the insufficient removal of telluric absorptions.

The results of the same kind of deconvolutions of HED meteorite reflectance spectra are shown in Fig. 2, and the optimized 1-μm absorption band parameters are listed in Table III. The residual errors of the deconvolutions are much smaller than those of the asteroids. Consequently, the errors of the 1-μm band parameters in Table III should be much smaller than those of the asteroids in Table II.

The 1-μm band parameters of the asteroids and meteorites are compared in Fig. 3. The points for the Vesta-like asteroids are plotted as filled squares with the estimated error bars, and those for HED meteorites as H, E, and D. The band centers of the asteroids and the meteorites seem to share the same center, and the asteroids cover a slightly wider range (6 of the 21 asteroids are out of the meteorite range). In the similar way, the band widths of the asteroids seem to cover a slightly wider range than the meteorites (8 of the 21 asteroids are out of the meteorite

TABLE II

The 1-μm Absorption-Band Centers, Widths, Strengths, the Root Mean Square Deviations (RMSD), and the Visible Absorption Strengths (V) Calculated from the Deconvolutions of Vesta-like Asteroids

Asteroid	Center (μm)	Width (μm)	Strength	RMSD	V
4 Vesta	0.9173(3)	0.174(3)	−0.416(10)	0.0090	0.22(5)
1273 Helma	0.9263(14)	0.238(13)	−0.602(27)	0.0279	0.52(13)
1906 Naef	0.9411(11)	0.218(8)	−0.338(15)	0.0144	1.05(12)
1929 Kolla	0.9254(5)	0.239(28)	−0.633(28)	0.0143	0.34(6)
1933 Tinchen	0.9101(5)	0.156(5)	−0.359(13)	0.0161	0.46(10)
2011 Veteraniya	0.9224(14)	0.217(15)	−0.500(33)	0.0329	0.60(17)
2113 Ehrdni	0.9162(11)	0.190(9)	−0.498(22)	0.0317	0.58(16)
2442 Corbett	0.9379(16)	0.263(17)	−0.815(46)	0.0426	0.38(14)
2590 Mourao	0.9177(5)	0.180(4)	−0.285(11)	0.0083	0.86(8)
3153 Lincoln	0.9264(12)	0.212(7)	−0.488(16)	0.0217	0.37(12)
3155 Lee	0.9111(5)	0.191(6)	−0.681(29)	0.0181	0.55(7)
3268 De Sanctis	0.9286(15)	0.165(6)	−0.317(5)	0.0276	0.69(22)
3657 1978 ST6	0.9162(3)	0.220(5)	−0.688(18)	0.0127	0.29(5)
3869 Norton	0.9240(11)	0.226(8)	−0.599(27)	0.0231	0.47(10)
3944 Halliday	0.9219(17)	0.197(8)	−0.400(16)	0.0242	0.61(15)
3968 Koptelov	0.9120(13)	0.165(7)	−0.323(15)	0.0282	0.48(19)
4005 1972 TC2	0.9318(10)	0.239(38)	−0.714(38)	0.0252	0.48(10)
4038 Kristina	0.9328(12)	0.184(5)	−0.374(8)	0.0197	1.11(18)
4147 Lennon	0.9095(11)	0.166(7)	−0.328(14)	0.0232	0.39(15)
4215 1987 VE1	0.9269(35)	0.194(12)	−0.522(21)	0.0378	0.60(17)
4546 Franck	0.9366(18)	0.230(12)	−0.351(18)	0.0176	0.64(14)

Note. The standard deviations of the band parameters are given as the last one or two digits in parentheses.

TABLE III

The 1-μm Absorption-Band Centers, Widths, Strengths, the Root Mean Square Deviations (RMSD), and the Visible Absorption Strengths (V) Calculated from the Deconvolutions of HED Meteorites

Meteorite	Center (μm)	Width (μm)	Strength	RMSD	V
ALHA76005	0.9332	0.1949	−0.6288	0.0031	0.3902
ALH78132	0.9294	0.1908	−0.6840	0.0030	0.3423
Juvinas	0.9346	0.2120	−0.8132	0.0048	0.1869
Millbillillie	0.9368	0.2139	−0.7483	0.0041	0.0970
Padvarninkai	0.9367	0.2021	−0.7387	0.0042	0.1623
Stannern	0.9351	0.1889	−0.6059	0.0039	0.2892
Y74450	0.9338	0.1993	−0.5622	0.0026	0.3303
EET87503	0.9296	0.1857	−0.5685	0.0029	0.1841
EETA79002	0.9191	0.1802	−0.8440	0.0033	0.0692
Johnstown	0.9173	0.1791	−0.6810	0.0028	0.1095
Y74013	0.9232	0.1671	−0.5942	0.0032	0.1318
Y75032	0.9258	0.1830	−0.7985	0.0027	0.1181

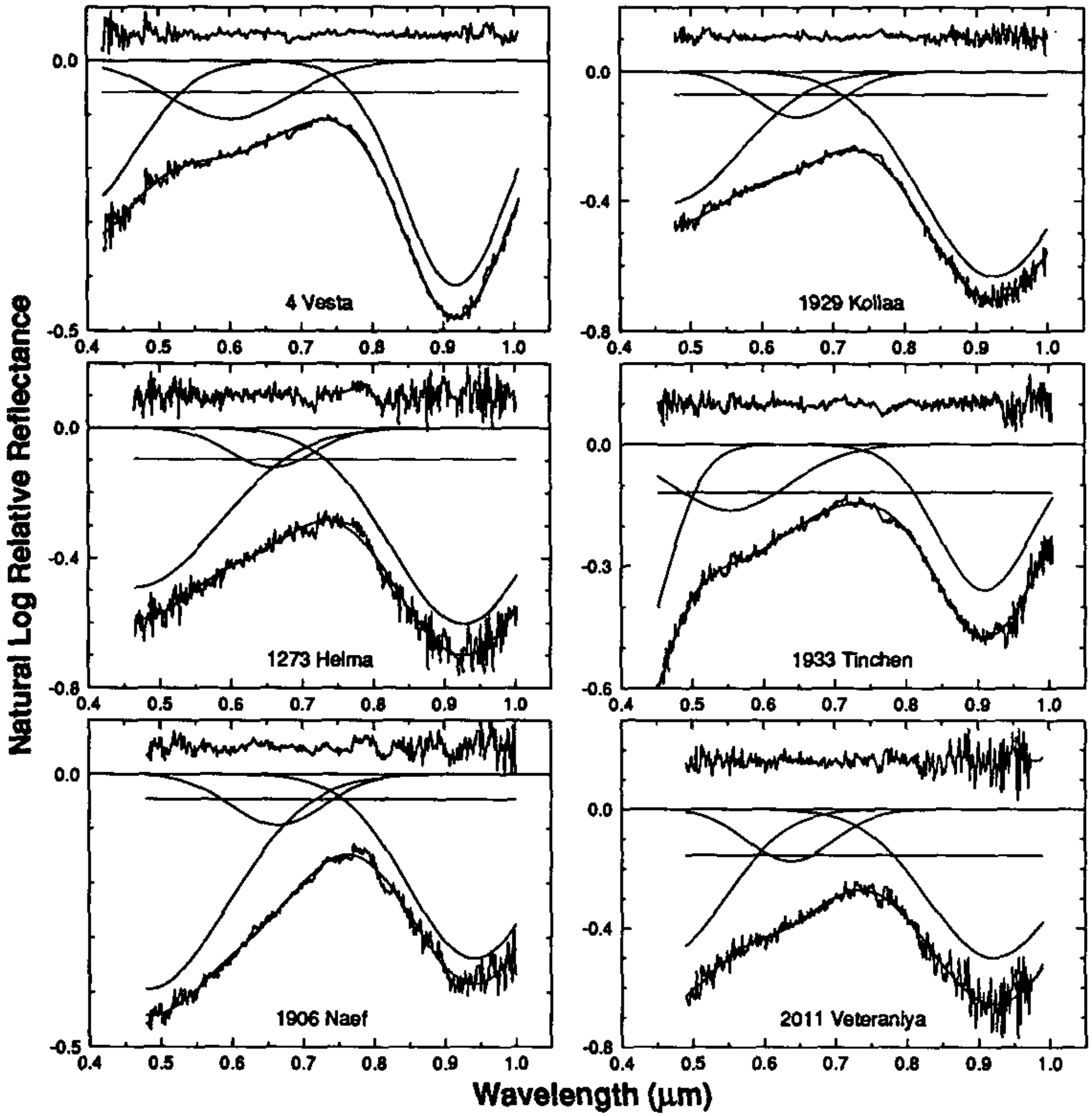

FIG. 1. Deconvolutions of reflectance spectra of 21 Vesta-like asteroids (including 4 Vesta) with a flat background and three Gaussians in the wavelength and natural logarithm space. Each vertical axis is shifted for an appropriate value. The residual error spectrum is shown above 0 line of each plot.

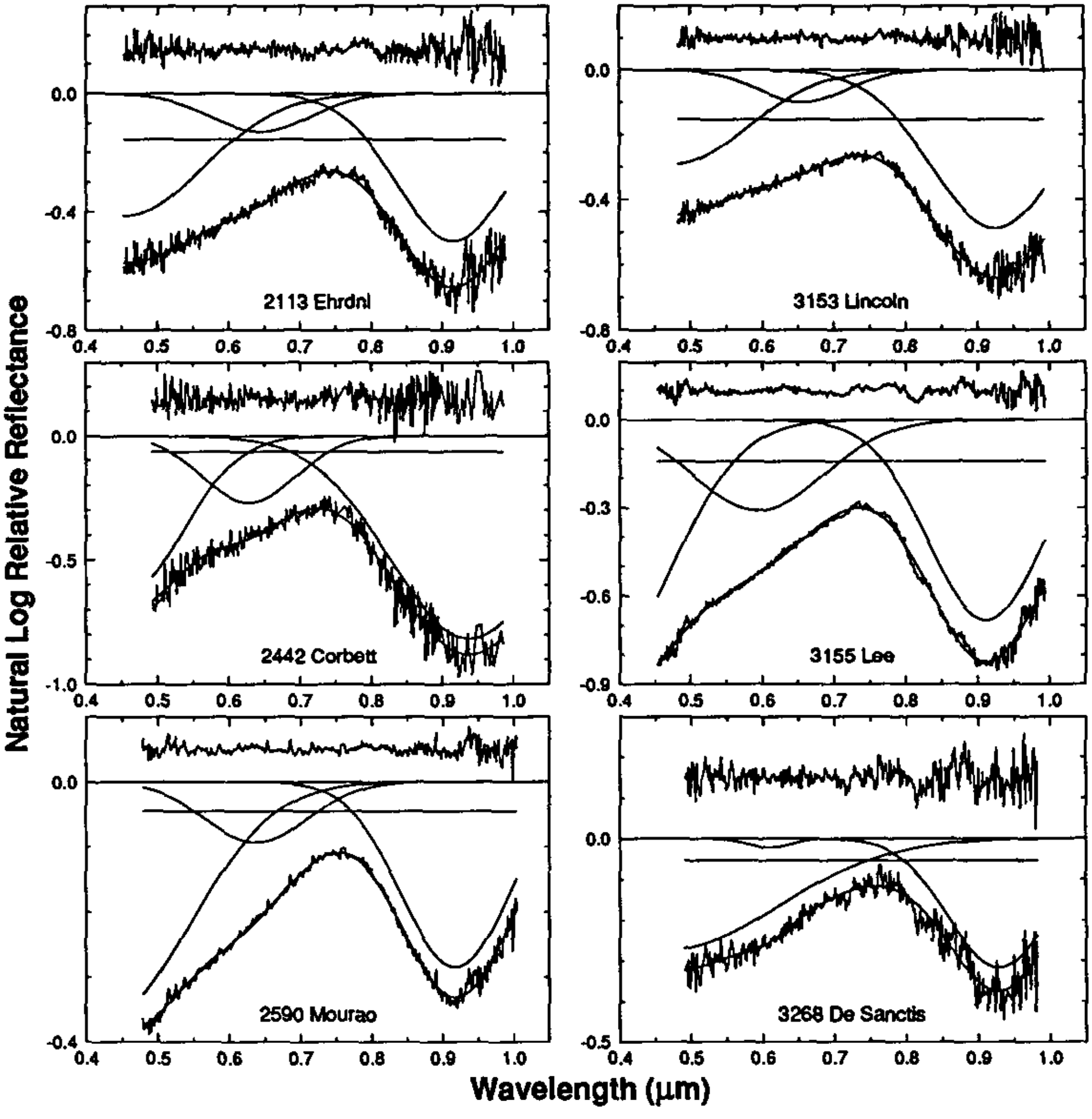

FIG. 1—*Continued*

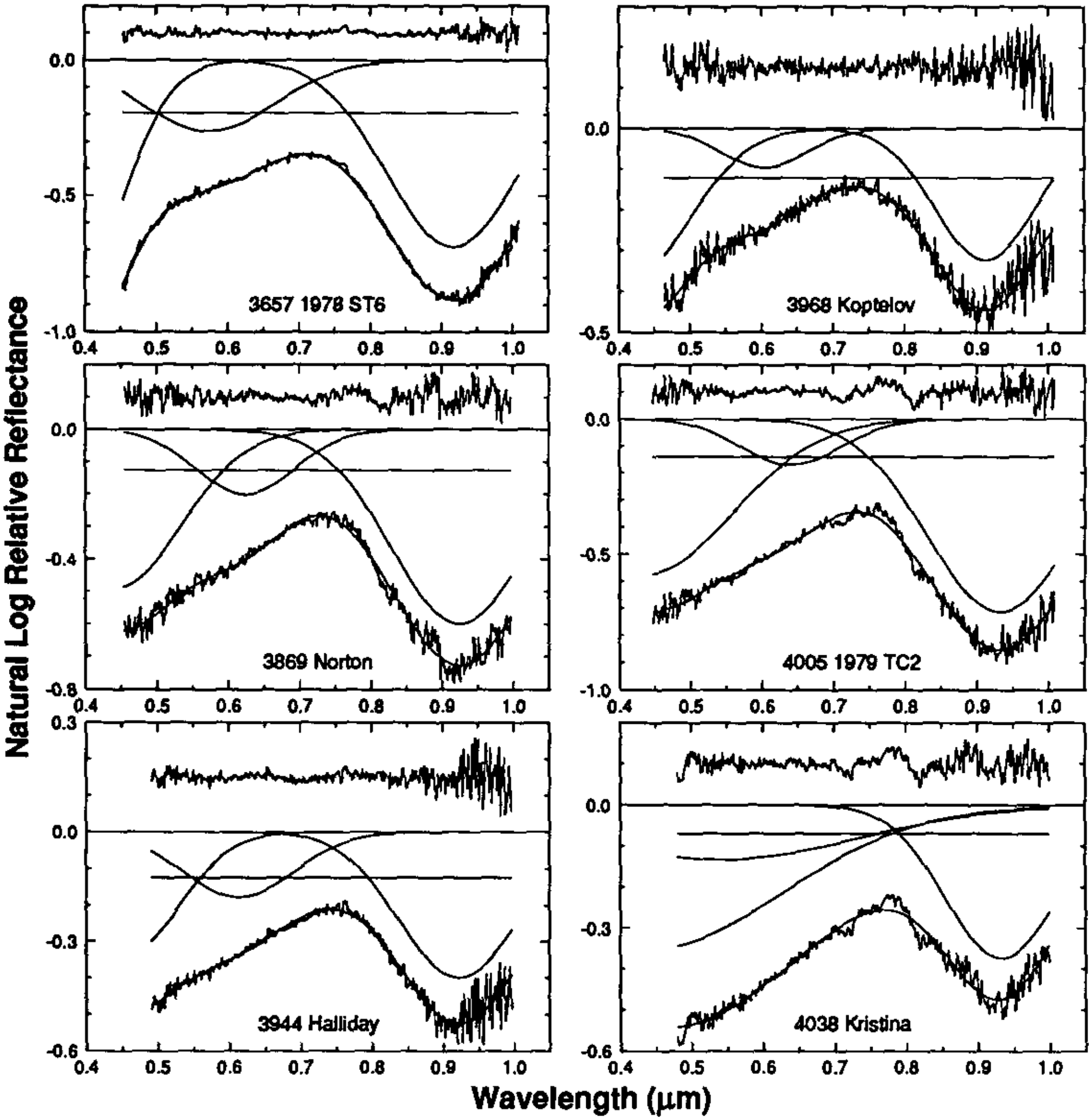

FIG. 1—*Continued*

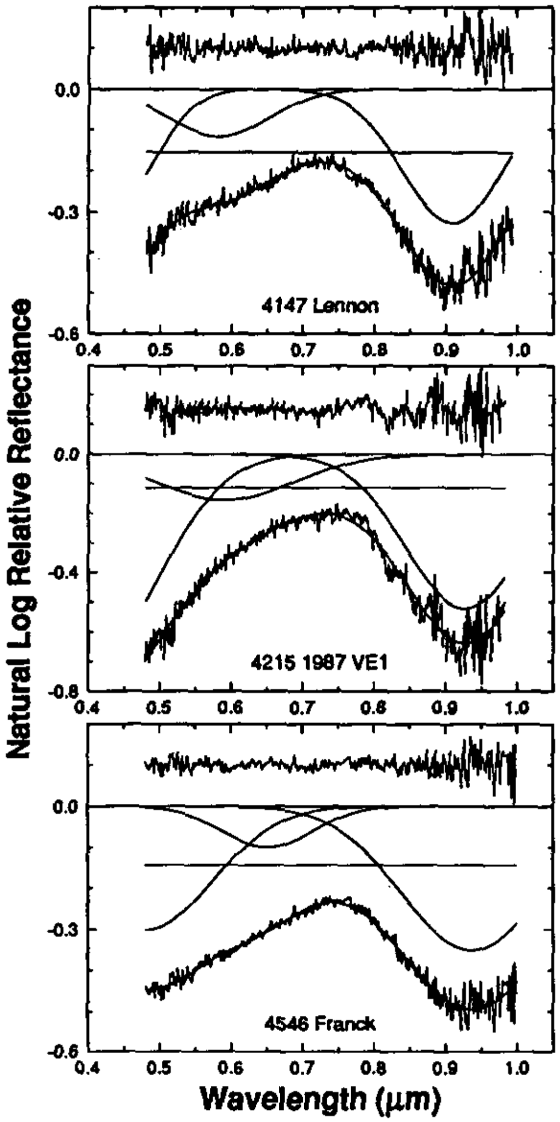

FIG. 1—*Continued*

range), and many of the asteroids have wider bands than the meteorites. On the other hand, band strengths of many of the Vesta-like asteroids are clearly weaker than HED meteorites. As many as 14 out of the 21 asteroids have weaker band strengths than the meteorites.

The visible absorption strength parameter V and the 1-μm band centers are plotted in Fig. 4. The visible absorption strengths of HED meteorites are always smaller than those of Vesta-like asteroids for the corresponding band center. Only some of the eucrite powders have band centers and visible absorption strengths relatively close to Vesta-like asteroids.

Two examples comparing the visible absorption strength of Vesta-like asteroids and HED meteorites are shown in Fig. 5. These two examples were chosen in order to show the similarity and difference between the Vesta-like asteroids and the HED meteorite spectra. Natural logarithm reflectance spectra of asteroids 4005 1979 TC2 and 3155 Lee are compared with those of Johnstown diogenite and ALHA76005 eucrite in Fig. 5a and 5b, respectively. These spectra are plotted with appropriate offsets so that they share the maximum point around 0.75 μm. Because ALH76005 has shallower 1-μm absorption band than 1979 TC2, the ALH76005 spectrum was scaled so that it has a similar 1-μm band strength to 1979 TC2 and is shown as a broken line in Fig. 5a. Overall match of their spectra is good except for the shoulder absorption around 0.81 μm, possibly due to telluric water. On the other hand, 3155 Lee has much stronger visible absorption than Johnstown, although they have nearly the same 1-μm band strength in Fig. 5b.

5. DISCUSSION

Hiroi *et al.* (1994) have shown that a particular howardite powder (EET87503) has a spectrum that is most similar to a particular set of measurements of Vesta's reflectance spectra constructed from the 8-color (Zellner *et al.* 1985), 24-color (Chapman and Gaffey 1979), and 52-color asteroid surveys (Bell *et al.* 1988). However, the high-resolution CCD spectrum of Vesta measured by Binzel and Xu (1993) is somewhat different from the same howardite powder. Perhaps this apparent discrepancy is because Vesta is known to have surface heterogeneity (Gaffey 1983) and the Vesta spectrum used by Hiroi *et al.* (1994) was a combination of broad to medium-width filter spectral observations performed at various rotational phases of Vesta.

The band center and width should provide mineralogical information if the deconvolution is accurate. However, the choices of the initial values of the background and the number of Gaussians to be used can affect the result to some extent. The band center wavelength is the least affected by such choices when a flat background is used. However, the bandwidth and strength can be somewhat influenced by the initial value of the background. In order to derive a consistent set of results, the maximum value of each spectrum around 0.74 μm was chosen as the initial background value as was mentioned earlier.

The slightly wider range of the 1-μm band centers of the Vesta-like asteroids than that of HED meteorites suggests either the band-center errors are underestimated or the asteroids have more variety of pyroxene chemical composition and/or olivine abundance than the meteorites studied. In the latter case, measurements of reflectance spectra of a greater number of HED meteorites might fill the gap between those asteroids and meteorites. Enrichment of olivine usually makes the 1-μm band wider and shift to longer wavelength.

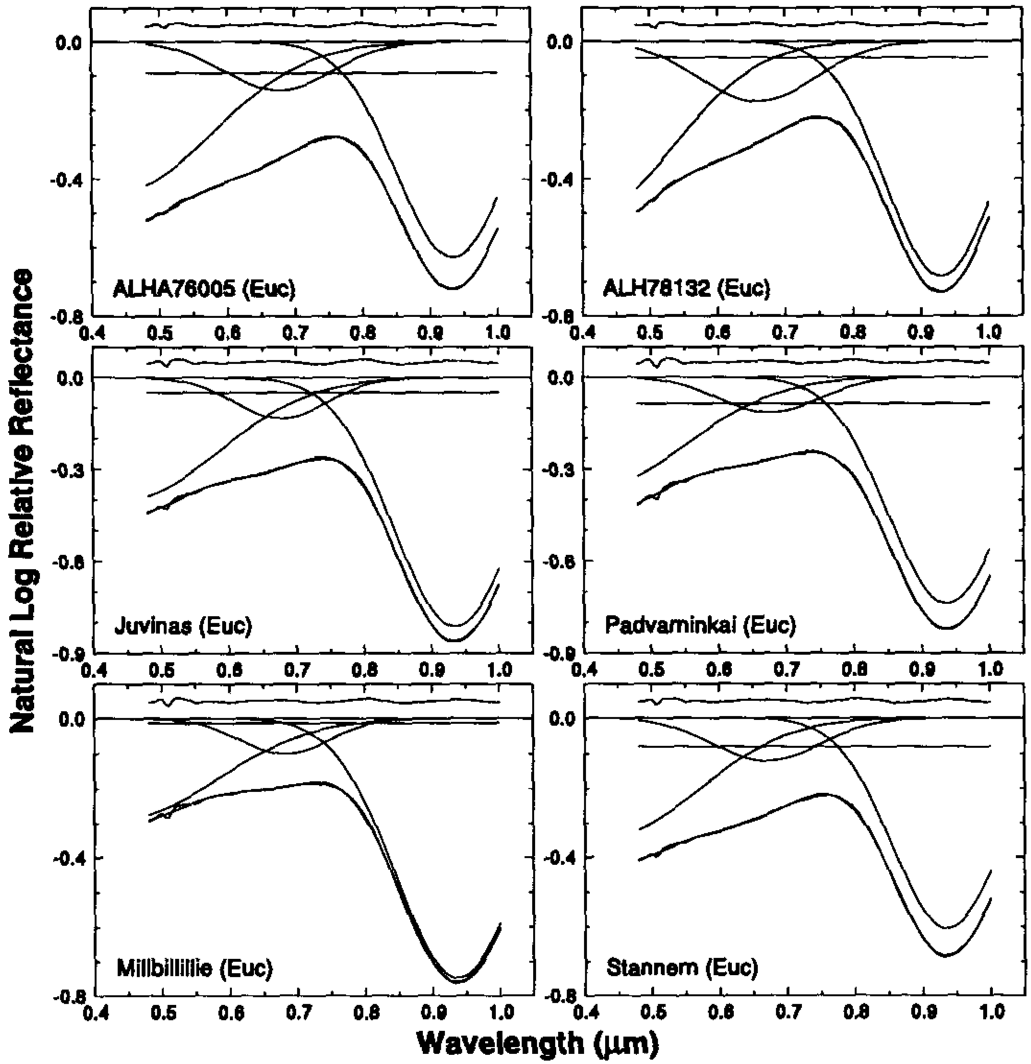

FIG. 2. Deconvolutions of reflectance spectra of 12 HED meteorite powders. The first three letters of class names are given in the parentheses.

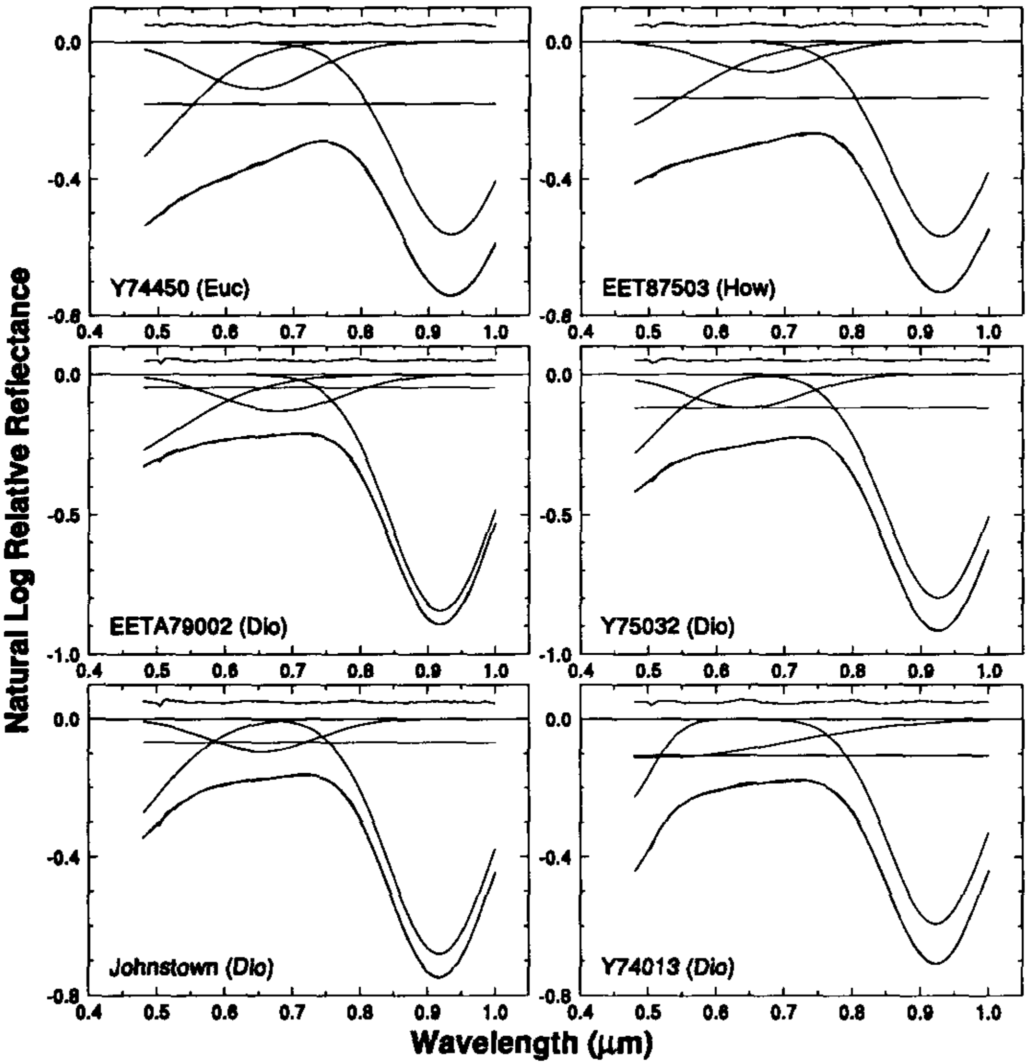

FIG. 2—*Continued*

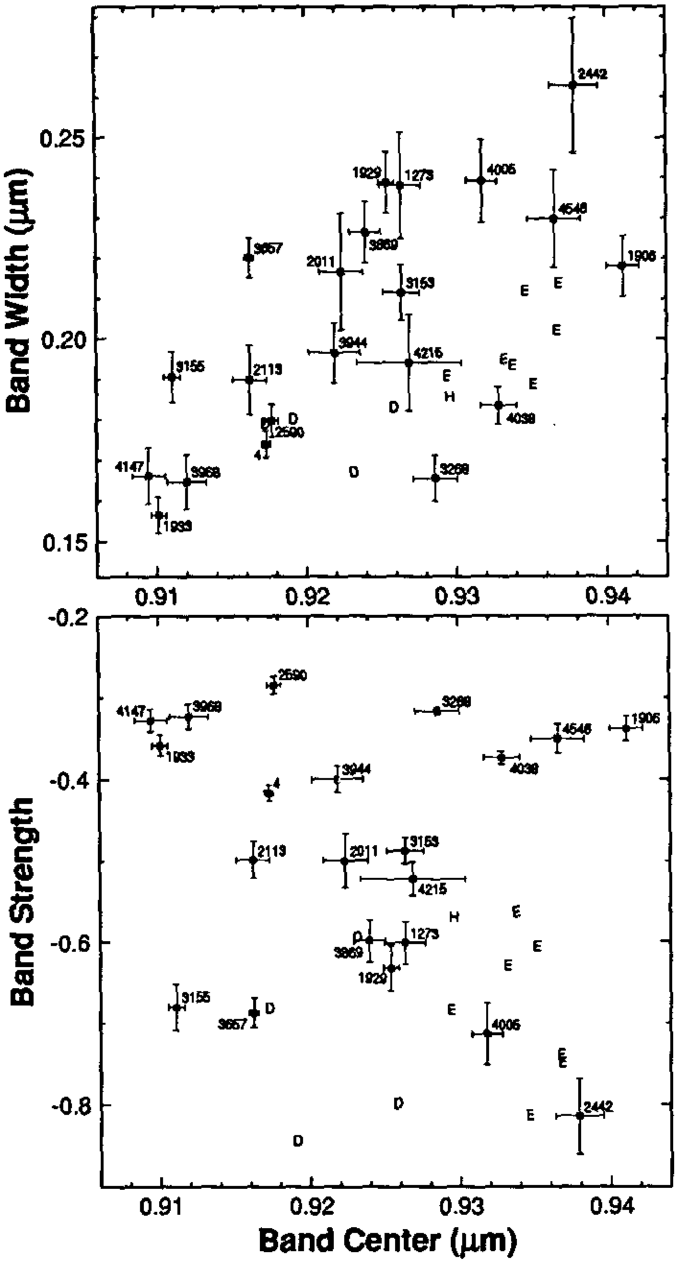

FIG. 3. Comparison of the 1-μm band centers, widths, and strengths between Vesta-like asteroids and HED meteorite powders. The asteroids points are plotted as filled squares, and HED meteorites as the first letters of the class names. The standard deviations of the asteroid points are given by bars.

The apparent slight difference of the bandwidths between the Vesta-like asteroids and HED meteorites may be due to a possible underestimation of the bandwidth errors. Even if the error estimations are correct, the bandwidth may appear different between the asteroids and meteorites if the initial background values are not appropriate.

On the other hand, the weaker band strengths of many of the Vesta-like asteroids than those of HED meteorites appear to be real. As shown in Fig. 3, there are many small Vesta-like asteroids that have stronger 1-μm bands than Vesta, which is consistent with the observations by Cruikshank *et al.* (1991). However, even the strongest 1-μm band of those asteroids is comparable to those of HED meteorite powders of grain size <25 μm. Because the band strengths of the asteroids seem to be independent of the band-center wavelengths in Fig. 3, the cause of their weaker band strengths must be (1) a larger amount of fine grains, (2) an enrichment of plagioclase that usually has no absorption band in the wavelength range of 0.9–0.95 μm, (3) some unidentified mineral components, or (4) accumulation of minor space weathering products in mineral grains. Because plagioclase has a weak absorption band around 1.2 μm, it may be possible to discriminate between the alternatives if reflectance spectra of Vesta-like asteroids can be measured well beyond 1.2 μm in wavelength as was done by Cruikshank *et al.* (1991). However, pyroxene also has a band around 1.2 μm due to Fe^{2+} in the M1 site, which makes the 1.2-μm band not unique.

The HED meteorites in this study were ground with a mortar and pestle and dry-sieved into the grain-size fractions of <25 μm. This procedure may have caused either a significantly different grain-size distribution from the asteroidal surfaces or a loss of extremely fine grains because of the nonvacuum environment of the laboratory. If such extremely fine grains can be retained among the regoliths on the Vesta-like asteroids (mostly 5–10 km in diameter), their weak 1-μm absorption band can be explained without much modification of mineral assemblage from the HED meteorites in this study.

An enrichment of plagioclase among the finest grain-size separate was observed for both lunar regolith and the experimental analogues impacted many times (Hörz and Cintala 1984). It is believed that the mechanical weakness of plagioclase relative to pyroxenes causes the enrichment of plagioclase among finer grains at each impact process. If that effect is working more effectively on the Vesta-like asteroids than the laboratory grinding process with a mortar and pestle, plagioclase grains on those asteroids become more dominant in their reflectance spectra, causing the apparently weaker 1-μm absorption band.

The parameter V for measuring the visible absorption strength in Eq. (5) was invented assuming that the visible absorption is some kind of volume absorption similar to the 1-μm band. If the visible absorption is not due to volume absorption, then normalization by the 1-μm absorption strength does not necessarily adjust for grain-size differences. The cause of the visible absorption bands of pyroxenes is not as well understood as the cause of the 1-μm absorption band. There are many possibilities: minor transition elements such as Ti, Cr, and Mn, and

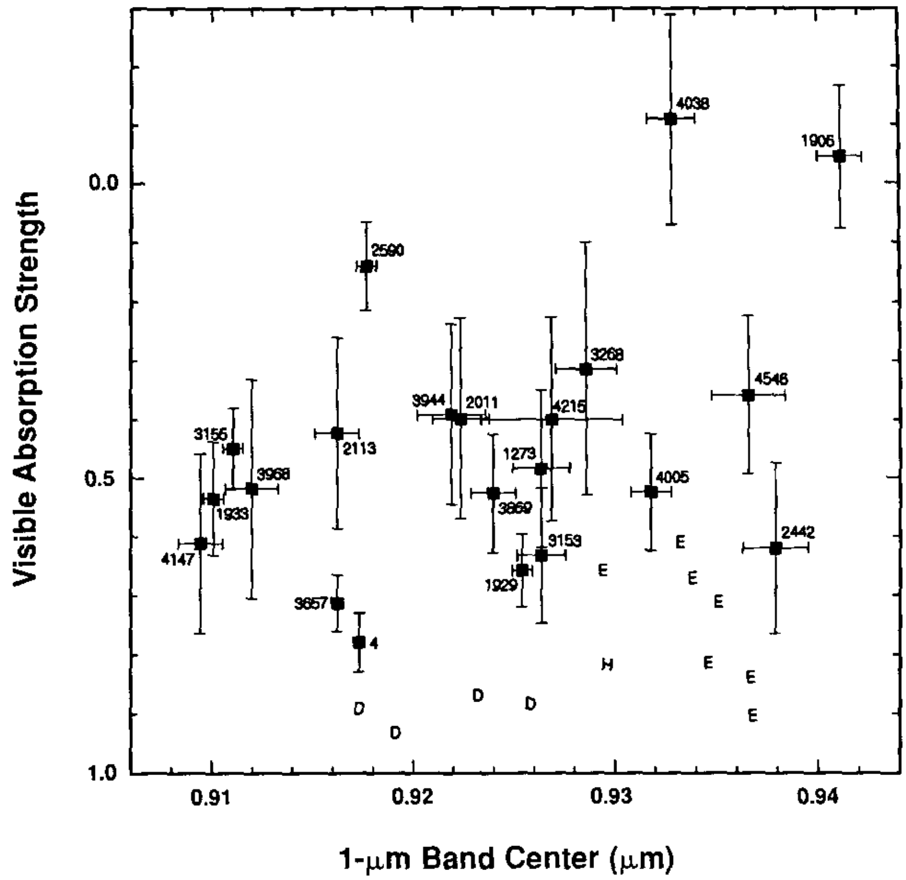

FIG. 4. Comparison of the 1-μm band centers and the visible absorption strengths (V) between Vesta-like asteroids and HED meteorite powders. The asteroids points are plotted as filled squares, and HED meteorites as the first letters of the class names. The standard deviations of the asteroid points are given by bars.

the oxidization state of Fe in pyroxene, other unidentified component minerals including metal, and space weathering. If Vesta-like asteroid surfaces were originally made of HED meteorite materials, then some form of alteration processes must have affected those asteroid surfaces. The general spectral differences of Vesta-like asteroids from HED meteorites, redder continuum and shallower absorption band, are consistent with lunar soils (Pieters *et al.* 1993). However, some asteroids (3155, 3657, 3869, 1929, and 1273) have redder continuum (stronger visible absorption) than the HED meteorites, but have similar absorption band strength as seen in Figs. 3b, 4, and 5b. This subject needs much more detailed analysis and basic research on the various causes of visible absorption for pyroxene and other minerals in general.

6. CONCLUSIONS

(1) Pyroxenes in the regolith of Vesta-like asteroids are similar to those in HED meteorites in chemical composition (Mg, Fe, and Ca contents).

(2) If the regoliths of Vesta-like asteroids are unweathered and compositionally similar to those of HED meteorites, many of those asteroids should be more fine grained or plagioclase-rich than the HED meteorite powders (<25 μm) prepared in this study.

(3) Stronger visible absorption for Vesta-like asteroids than for HED meteorites suggests (a) differences in minor elemental contents or Fe oxidization state in pyroxene, (b) existence of additional unidentified mineral components, or (c) minor space weathering on those asteroids.

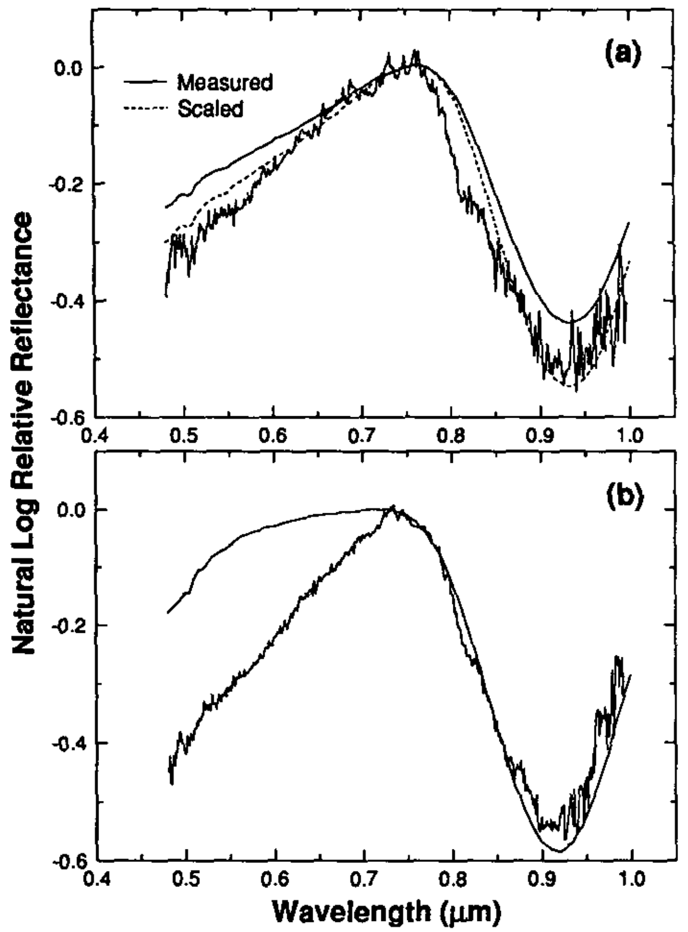

FIG. 5. Two examples of comparison of reflectance spectra between Vesta-like asteroids and HED meteorite powders. Measured natural logarithm reflectance spectra are shown in solid lines with appropriate offsets so that they share the maximum point around 0.75 μm. (a) Asteroid 4005 1979 TC2 and ALHA76005 eucrite. The ALHA76005 spectrum was also scaled so that it has a similar 1-μm band strength to 1979 TC2 and is plotted in a broken line. (b) Asteroid 3155 Lee and Johnstown diogenite.

ACKNOWLEDGMENTS

We thank E. A. Cloutis and an anonymous referee for their constructive comments. Antarctic meteorites were loaned from the Meteorite Working Group and the National Institute of Polar Research. Juvinas eucrite was loaned from the Field Museum of Natural History, and the other HED meteorites from the Planetary Materials Database Collections of Mineralogical Institute, University of Tokyo. We thank A. Yamaguchi for the chemical compositions of some eucrites. Reflectance spectra of the above meteorites were measured at RELAB in Brown University. We thank S. F. Pratt for the measurements. RELAB is a multiuser facility operated under NASA Grant NAGW-748. This work was done while T.H. held a National Research Council Research Associateship and was supported by NASA Planetary Astronomy Program at NASA Johnson Space Center. T.H. also appreciates constant support by F. Vilas.

REFERENCES

Bell, J. F. 1988. An Earth-crossing source body for the basaltic achondrites: Vesta's son or Vesta's nephew? *Lunar Planet. Sci.* **19,** 55–56.

Bell, J. F., P. D. Owensby, B. R. Hawke, and M. J. Gaffey 1988. The 52-color asteroid survey: Final results and interpretation. *Lunar Planet. Sci.* **19,** 57–58.

Binzel, R. P., and S. Xu 1993. Chips off of asteroid 4 Vesta: Evidence for the parent body of basaltic achondrite meteorites. *Science* **260,** 186–191.

Chapman, C. R., and M. J. Gaffey 1979. Reflectance spectra for 277 asteroids. In *Asteroids* (T. Gehrels, Ed.), pp. 1064–1089. Univ. of Arizona Press, Tucson.

Cruikshank, D. P., D. J. Tholen, W. K. Hartmann, J. F. Bell, and R. H. Brown 1991. Three basaltic Earth-approaching asteroids and the source of the basaltic meteorites. *Icarus* **89,** 1–13.

Dollfus, A., J. E. Geake, J.-C. Mandeville, and B. Zellner 1977. The nature of asteroid surfaces from optical polarimetry. In *Comets, Asteroids, Meteorites* (A. H. Delsemme, Ed.), pp. 243–261. Univ. of Toledo Press, Toledo.

Dollfus, A., M. Wolff, J. E. Geake, D. F. Lupishko, and L. M. Dougherty 1989. Photopolarimetry of asteroids. In *Asteroids II* (R. P. Binzel, T. Gehrels, and M. S. Matthews, Eds.), pp. 594–616. Univ. of Arizona Press, Tucson.

Gaffey, M. J. 1983. The asteroid (4) Vesta: Rotational spectral variations, surface material heterogeneity, and implications for the origin of the basaltic achondrites. *Lunar Planet. Sci.* **14,** 231–232.

Hiroi, T., C. M. Pieters, and H. Takeda 1994. Grain size of the surface regolith of asteroid 4 Vesta estimated from its reflectance spectrum in comparison with HED meteorites. *Meteoritics* **29,** 394–396.

Hörz, F., and M. J. Cintala 1984. Grain size evolution and fractionation trends in an experimental regolith. *Proc. Lunar Planet. Sci. Conf. 15th,* C183–C196.

Huguenin, R. L., and J. L. Jones 1986. Intelligent information extraction from reflectance spectra: Absorption band positions. *J. Geophys. Res.* **91,** 9585–9598.

Le Bertre, T., and B. Zellner 1980. Surface texture of Vesta from optical polarimetry. *Icarus* **43,** 172–180.

McCord, T. B., J. B. Adams, and T. V. Johnson 1970. Asteroid Vesta: Spectral reflectivity and compositional implications. *Science* **168,** 1445–1447.

McFadden, L. A., M. J. Gaffey, and T. B. McCord 1984. Mineralogical-petrological characterization of near-Earth asteroids. *Icarus* **59,** 25–40.

Pieters, C. M. 1983. Strength of mineral absorption features in the transmitted component of near-infrared reflected light: First results from RELAB. *J. Geophys. Res.* **88,** 9534–9544.

Pieters, C. M., E. M. Fischer, O. Rode, and A. Basu 1993. Optical effects of space weathering: The role of the finest fraction. *J. Geophys. Res.* **98,** 20,817–20,824.

Rossman, G. R. 1980. Pyroxene spectroscopy. *Rev. Mineral.* **7,** 93–116.

Score, R., and M. M. Lindstrom 1990. *Antarct. Meteorite Newsl.* **13**(1).

Sunshine, J. M., C. M. Pieters, and S. F. Pratt 1990. Deconvolution of mineral absorption bands: An improved approach. *J. Geophys. Res.* **95,** 6955–6966.

Sunshine, J. M., and C. M. Pieters 1993. Estimating modal abundances from the spectra of natural and laboratory pyroxene mixtures using the modified Gaussian model. *J. Geophys. Res.* **98,** 9075–9087.

TAKEDA, H., A. M. REID, AND T. YAMANAKA 1975 Crystallographic and chemical studies of a bronzite and chromite in the Yamato (B) achondrite. *Mem. Natl. Inst. Polar Res. Spec. Issue* **5,** 83–90.

YANAI, K., AND H. KOJIMA 1987. *Photographic Catalog of the Antarctic Meteorites.* National Institute of Polar Research, Tokyo.

Zellner, B., D. J. Tholen, and E. F. Tedesco 1985. The eight-color asteroid survey: Results for 589 minor planets. *Icarus* **61,** 355–416.